Charge Separation Kinetics in Intact Photosystem II Core Particles Is Trap-Limited. A Picosecond Fluorescence Study†

Y. Miloslavina,‡ M. Szczepaniak,‡ M. G. Müller,‡ J. Sander,# M. Nowaczyk,# M. Rögner,# and A. R. Holzwarth*,‡

Max-Planck-Institut für Bioanorganische Chemie, Stiftstrasse 34−36, D-45470 Mülheim a.d. Ruhr, Germany, and Lehrstuhl für Biochemie der Pflanzen, Ruhr-Universität Bochum, Universitätsstrasse 150, D-44801 Bochum, Germany

Received November 3, 2005; Revised Manuscript Received December 10, 2005

ABSTRACT: The fluorescence kinetics in intact photosystem II core particles from the cyanobacterium *Thermosynechococcus elongatus* have been measured with picosecond resolution at room temperature in open reaction centers. At least two new lifetime components of ≈2 and 9 ps have been resolved in the kinetics by global analysis in addition to several known longer-lived components (from 42 ps to ≈2 ns). Kinetic compartment modeling yields a kinetic description in full agreement with the one found recently by femtosecond transient absorption spectroscopy [Holzwarth et al. (2005) submitted to *Proc. Natl. Acad. Sci. U.S.A.*]. We have for the first time resolved directly the fluorescence spectrum and the kinetics of the equilibrated excited reaction center in intact photosystem II and have found two early radical pairs before the electron is transferred to the quinone Q_A. The *apparent lifetime* for primary charge separation is 7 ps, that is, by a factor of 8−12 faster than assumed on the basis of earlier analyses. The main component of excited-state decay is 42 ps. The effective primary charge separation rate constant is 170 ns^{-1}, and the secondary electron-transfer rate constant is 112 ns^{-1}. Both electron-transfer steps are reversible. Electron transfer from pheophytin to Q_A occurs with an apparent overall lifetime of 350 ps. The energy equilibration between the CP43/CP47 antenna and the reaction center occurs with a main *apparent lifetime* of ≈1.5 ps and a minor 10 ps lifetime component. Analysis of the overall trapping kinetics based on the theory of energy migration and trapping on lattices shows that the charge separation kinetics in photosystem II is extremely trap-limited and not diffusion-to-the-trap-limited as claimed in several recent papers. These findings support the validity of the assumptions made in deriving the earlier exciton radical pair equilibrium model [Schatz, G. H., Brock, H., and Holzwarth, A. R. (1988) *Biophys. J. 54*, 397−405].

Photosystem (PS)[1] II is responsible in oxygenic photosynthesis for water splitting and for providing reduction equivalents to reduce $P700^+$ of PS I. The structure of PS II from cyanobacteria has recently been determined by X-ray diffraction to a resolution of 3.2−3.5 Å (*1*−*5*). The PS II core consists of the antenna polypeptides CP43 and CP47, which carry 13 and 16 chlorophyll (Chl) *a* molecules, respectively, organized in two layers located near the cytoplasmic and the lumenal sides of the membrane. Furthermore, they contain the D1/D2-cyt-b559 reaction center (RC) polypeptides, which carry the cofactors of the electron-transfer chain [four Chls, two pheophytins (Pheo), and two quinones] and two additional antenna Chls (the so-called peripheral Chl_z^{D1} and Chl_z^{D2} molecules), which are located ≈25 Å apart from the pigments of the electron-transfer chain. In the native state PS II cores occur as dimers (*6*). The initial processes are light absorption in the antenna, followed by energy transfer to the RC in which ultrafast photon-induced charge separation across the membrane occurs. Eventually the oxygen-evolving complex is oxidized by the RC cofactors and water-splitting occurs at a tetranuclear manganese complex (see ref *7* for a recent review on electron-transfer processes in PS II).

The energy transfer and charge separation kinetics in intact PS II core particles were studied about two decades ago by time-resolved fluorescence and transient absorption with a resolution of ≈10 ps (*8*−*10*). Dominant lifetime components with open RCs (i.e., the F_0 state) were observed in the range from 35 ps (*8*) to 60−80 ps (*10*), depending on the method used, which was ascribed to antenna trapping by primary charge separation and ≈300−500 ps, which was assigned to secondary electron transfer to the quinone acceptor Q_A (*8*−*10*). These data subsequently gave rise to the development of a kinetic model for the early energy- and electron-transfer processes in PS II cores, which became known as the "exciton/radical pair equilibrium model" (ERPE model) (*9*). The ERPE model has been used extensively in the field to analyze and explain a wide range of phenomena related to the kinetics of the early processes in PS II such as radical pair formation, its dependence on the redox states of the

† This research was supported in part by the European Union Research and Training Network "Intro2", Human Resources and Mobility Activity, contract MRTN-CT-2003-505069, by the Project "Samba per 2", Regional Development Fund, Trento Region, Italy, and by the Deutsche Forschungsgemeinschaft (DFG, SFB 480, Ruhr-Universität Bochum).

* Corresponding author [telephone (+49) 208 306 3571; fax (+49) 208 306 3951; e-mail holzwarth@mpi-muelheim.mpg.de].

‡ Max-Planck-Institut für Bioanorganische Chemie.

Ruhr-Universität Bochum.

[1] Abbreviations: RC, reaction center; PS, photosystem; Chl, chlorophyll; DAS, decay-associated (emission) spectrum; Pheo, pheophytin; RP, radical pair; β-DM, *n*-dodecyl-β-D-maltoside; MES, 2[*N*-morpholino]ethanesulfonic acid; SAS, species-associated (emission) spectrum.

10.1021/bi052248c CCC: $33.50
Published on Web 01/28/2006

cofactors, and Chl quenching in the antenna and the RC. The ERPE model made the hypothesis that internal energy equilibration within the PS II core antennae and from the antennae to the RC should occur on a time scale of a few picoseconds (*9*), that is, below the ≈10 ps resolution of the time-resolved experiments at the time (actually an equilibration time of ≤3 ps was estimated). It was therefore assumed in the ERPE model that the charge separation would start from an equilibrated excitation state distributed over both the antenna and the RC pigments. Consequently, no details of the energy-transfer processes were considered in the model. This assumption gave rise to a relatively simple and straightforward description of the excited-state dynamics, which resulted in a biexponential decay and overall trap-limited charge separation kinetics (*9*).[2] The time scale of this energy equilibration process is, however, of central importance for recent discussions which, on the basis of the relatively large distance of 14−17 Å from the antenna Chls to the RC pigments (*2*), questioned the possibility of an energy equilibration on a time scale faster than primary charge separation (*11*, *12*). In fact, it was concluded in these papers that energy transfer to the RC was slow as compared to primary charge separation. Consequently, it has been concluded by Vasil'ev et al. as well as other authors that the ERPE model is inadequate to describe the charge separation and trapping dynamics in PS II and that the kinetics is in fact "transfer-to-the-trap-limited" (*12*, *13*). The latter conclusion implies that the transfer from the antenna to the RC pigments is the rate-limiting step rather than charge separation. In view of this controversial situation a clarification of the rate of the energy-transfer processes in relation to the rates of the electron-transfer processes in intact PS II particles is required. Interestingly, recent time-resolved fluorescence data on intact core particles (*11*, *12*) did not reveal any components faster than the ≈40−60 ps process reported much earlier (*8*−*10*). Yet, very recent transient absorption measurements on the intact PS II cores revealed much faster components (*14*). Similarly, time-resolved experiments on smaller systems, such as the CP47/D1-D2 complex, revealed also faster lifetime components on the time scale of a few picoseconds and 10−20 ps (*15*). However, the assignment of the various lifetime components to energy-transfer and/or charge separation processes in these systems is also under debate.

Another controversial discussion that has come up recently concerns the question of whether the rates and the mechanism of the early electron-transfer processes in intact PS II cores and in isolated D1/D2-cyt-b559 RCs are identical or not. Whereas we estimated very similar intrinsic rate constants for the primary charge separation in intact PS II cores (*9*) and in D1-D2 RCs (*16*), the identity of these processes in the two systems has also been questioned recently (*11*, *12*) (for recent reviews see refs *7* and *17*). In view of this situation we aim in the present work to provide new fluorescence kinetic data on intact PS II cores that complement the recent transient absorption kinetics and are suitable for an improved kinetic modeling of the energy- and electron-transfer processes in PS II. We will in particular address the question of "transfer-to-the-trap-limited" (i.e., diffusion-limited) versus "trap-limited" kinetics.

[2] We note here in passing that recently in the literature the typical excited-state equilibration time that was assumed in the derivation of the "exciton/radical pair equilibrium model" has been misquoted to be in the range of a few hundreds of femtoseconds (*15*), i.e., by an order of magnitude shorter than the ≤3 ps value that had actually been assumed (*9*).

MATERIALS AND METHODS

Time-resolved fluorescence measurements have been performed at room temperature on dimeric PS II core particles from *Thermosynechococcus elongatus* (*T. elongatus*) with intact oxygen evolution isolated and purified according to ref *18*. These particles showed an average oxygen evolution rate of 3200 (± 10%) μmol of O_2/(mg of Chl)/h. Fluorescence measurements have been performed in a buffer of 20 mM MES (pH 6.5), containing 500 mM mannitol, and ferricyanide (0.4 mM) was added to keep the RC in an open (F_0) state. To ensure that no significant amount of closed RCs was present, the sample was kept in a rotating (4000 rpm) cuvette of 1.5 mm path length with a diameter of 10 cm, which was also oscillated sideways with 66 rpm. Stopping the movement (and thus allowing RCs to close) of the cuvette led to an increase by a factor of 11−12 in the fluorescence intensity. The laser excitation intensity was low enough to ensure that during a single passage of the sample volume through the laser beam the excitation probability for a PS II particle was < ≈50%. Fluorescence kinetics was detected by a single-photon-counting apparatus, which allows measurements with a resolution of 1−2 ps, as described elsewhere (*19*, *20*). Initial kinetic analysis has been performed by global lifetime analysis (*21*). Subsequent global compartment modeling has been used to test and compare various kinetic models directly on the original data (not on the results of the global lifetime analysis). Advantages of the latter kind of analysis have been discussed previously (*20*−*22*).

RESULTS

An excitation wavelength of 663 nm, located in the blue absorbing edge of the Q_y band of the Chl antenna, has been chosen. This excites preferentially the CP43 complex (*23*, *24*). Fluorescence kinetics has been measured with a high signal/noise ratio (30000 counts in the peak channel at all wavelengths) at 4 nm intervals in the range from 673 to 701 nm with very low excitation intensity ($<10^{-4}$ absorbed photons/particle/pulse). Extreme care has been taken to avoid re-excitation of the same particle before reopening of the RC. Thus, the measured kinetics reflects >99% open RCs (see Materials and Methods for details).

For a good description of the kinetics across the whole wavelength range 6 lifetimes were required in global analysis over a fitting range of 2 ns [cf. Figure 1 for the decay-associated spectrum (DAS)]. The lifetimes with dominant amplitude were 2, 9, 42, 106, and 332 ps. An additional lifetime of 2 ns with a very small amplitude was also required. The χ^2 value for this global fit was 1.07. Leaving out the shortest lifetime component from the fit worsened the χ^2 value drastically to 1.15 and led to large deviations in the residual plots (the data for six- and five-component analyses are given in the Supporting Information). Whereas the longer lifetimes, including the ≈40 ps component, have been resolved earlier in the fluorescence kinetics of intact PS II cores (*9*−*12*), the two faster lifetimes of 2 and 9 ps have not been resolved before.

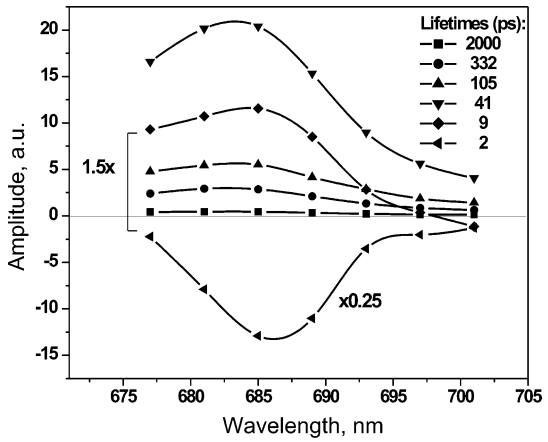

FIGURE 1: Decay-associated emission spectra (DAS) of PS II core particles from *T. elongatus* excited at 663 nm as analyzed by global lifetime analysis.

The amplitude of the fastest lifetime component is negative across the whole wavelength range with a minimum around 685 nm and approaches zero near 675 nm. At slightly shorter detection wavelengths a positive amplitude has been observed for this component. However, we did not include these short-wavelength data in the present fit because below 676 nm we cannot exclude a scattering contribution from the exciting pulse. The amplitudes of all other lifetime components are positive across the whole spectrum with peaks around 680−685 nm, except for the 9 ps component, which is also slightly negative at the longest detection wavelength. The fastest component (≈2 ps) clearly shows the amplitude feature of an energy-transfer process, and we assign it to a mixture of both energy transfer within the antenna complexes CP43 and CP47 (*25*) and to energy transfer from the antenna complexes to the RC, in agreement with recent femtosecond transient absorption data on the same system (*14*) (vide infra for a detailed discussion). All longer lifetime components must be assigned to energy trapping by primary charge separation and to secondary electron-transfer processes, which can be observed in the Chl fluorescence decay due to the charge recombination processes active in PS II (*9, 20*). The assignment of the ≈330 ps process is likely electron transfer from $Pheo^-$ to Q_A (*9*). Strictly speaking, each of the lifetimes, which are the inverse eigenvalues of the kinetic matrix of the system, depends on all rate constants in the system and generally does not reflect the property of a particular excited-state species or radical pair intermediate. For this reason an interpretation in terms of lifetime components can provide at best a qualitative interpretation, and a detailed kinetic modeling is required to get physical insight into the kinetics of the system.

KINETIC MODELING

We have applied global compartment modeling to the kinetics by testing several different kinetic models on the data. The simplest kinetic scheme that allowed a good description of the experimental data is shown in Figure 2 together with the optimal rate constants from a global target modeling. The system contains five compartments, that is, three excited-state compartments (CP43*, CP47*, and RC*) and two radical pair compartments (RP1 and RP2). RC* stands for the equilibrated excited state of the six pigments comprising the RC. The species-associated emission spectra

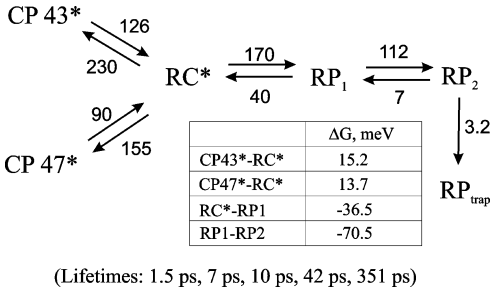

FIGURE 2: Kinetic model for dimeric PS II core particles resulted from target analyses. Rate constants are given in ns^{-1}. Errors of electron-transfer rates are ±10%, whereas errors in energy-transfer rates may be up to ±20% due to the lifetime of 1.5 ps being close to the resolution limit of the apparatus. Lifetimes resulting from the model are shown at the bottom. (Inset) Free energy differences ΔG between compartments as calculated from the forward and backward rates of energy or electron transfer.

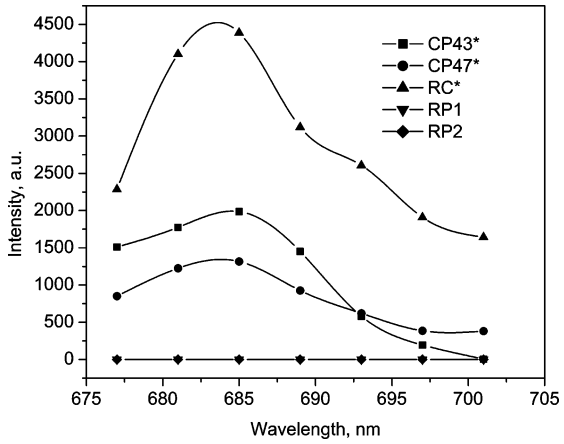

FIGURE 3: Species-associated emission spectra (SAS) resulting from the fit of the kinetic model present in Figure 2 to the data.

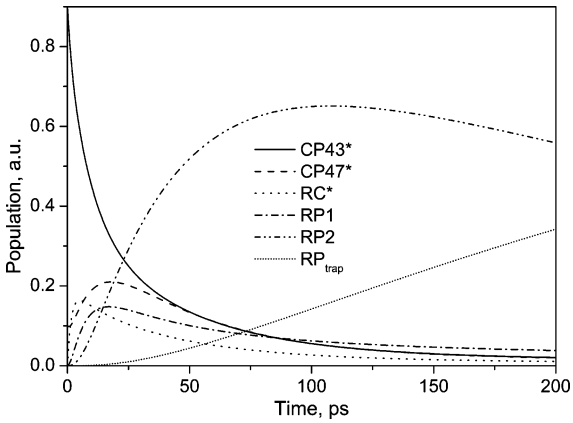

FIGURE 4: Calculated time dependence of populations of the compartments as shown in Figure 2.

(SAS) of the compartments are given in Figure 3, and the time-dependence of the populations of the compartments is shown in Figure 4. The SAS of radical pairs are zero by definition, because RPs are not fluorescent. Nevertheless, the kinetics of the RP states is observed in fluorescence indirectly by way of the charge recombination fluorescence because both early electron-transfer steps are reversible.

This kinetic scheme results in lifetime components of 1.5, 7, 10, 42, and 351 ps. In the modeling two additional free running lifetime components of 111 ps and 2.3 ns of small amplitude were required for a good fit (see Figure 7 for the

corresponding DAS). Thus, all lifetime components from the global analysis are present in this model. However, the 9 ps lifetime from global analysis is now split into two components of 7 and 10 ps, which would be too close-lying to be resolved in global analysis. The small 2.3 ns component is clearly due to a very small amount of closed RCs in the sample, whereas the origin of the 111 ps component, which is outside the kinetic scheme shown in Figure 2, is unclear at present. Thus, there is possibly room for a slightly extended or more complex model (vide infra). Other and/or simpler kinetic schemes than the one shown in Figure 2 either did not result in a good fit to the data or did not provide any reasonable SAS or both.

DISCUSSION

The kinetic scheme giving a good fit to the data is analogous to the one found earlier explaining the femtosecond transient absorption data (*14*). The rate constants for the electron-transfer processes are in fact the same within the error limits as found for transient absorption. Also, the rate constants of energy transfer are very similar, except for a slight difference in the rate constant of forward energy transfer from CP43 to the RC, which is somewhat higher in transient absorption than in the fluorescence model.

We believe, however, that the 111 ps component (contributing ≈10% to the relative amplitude) is outside of our present kinetic model and that it most likely derives from the intact PS II core system, unless we assume some heterogeneity. If one wants to include such a 111 ps component, the kinetic scheme has to be extended beyond the one shown in this paper. From the expected rate constant of a process giving rise to a 111 ps component (somewhere in the range of $6-9\ ns^{-1}$) one can conclude that this should be a process that happens after formation of the second radical pair but before the electron transfer to Q_A. We have tested various such extended models on our fluorescence data but could not come to a clear conclusion as to the origin of the 111 ps component. One likely possibility would be that this component reflects a protein relaxation step after formation of RP2 and before the electron transfer to Q_A. Protein relaxation steps have been described for PS II cores and RCs by various authors, including ourselves (see, e.g., refs *11* and *16*). The upshot is that the model presented here should be considered as a minimal model that provides a very good description for the mechanism and rates of the electron-transfer steps (note that any potential further electron-transfer step should have shown up in the transient absorption data), but might have to be extended later to include some protein relaxation as well.

The important conclusion for the present paper—and that is the result from all our modeling of more extended kinetic schemes—is, however, that whatever extension in the kinetic scheme is made, it does not change to any significant extent the rate constants of the energy-transfer processes between antenna and RC or the rate constants of the early electron-transfer step(s). Because the focus of the present paper is primarily on the clarification of the trap- versus diffusion-limited model and of the rate constant [and *apparent lifetime* (for clarification of the kinetic terms, see ref *20*)] of the primary charge separation, any further extension of the kinetic scheme would not affect in any way our conclusions drawn in this paper (or the rate constants in Figure 2 for the processes up to and including the rate constants for the formation of RP2).

The weighted eigenvectors corresponding to the kinetic scheme in Figure 2 are given in Table 1. This eigenvector matrix allows one to assign the origin of the various lifetimes in the model to the physical processes and the compartment kinetics. A negative value indicates a rise of a compartment population, and a positive value indicates a decay. Generally, the lifetimes are functions of all rate constants in the model. Thus, there is essentially some contribution of all lifetimes to each of the compartment populations. However, we are looking here only for the amplitudes that make the dominant contributions to the various compartment populations. It can be clearly seen from Table 1 that the 1.5 ps lifetime represents primarily the rise of the RC* population; that is, it is the dominant component describing the energy-transfer kinetics from the antennae to the RC besides a very small contribution to the RC* rise by the 7 ps lifetime. Thus, the overall equilibration time between antenna and RC should be in the range of a few picoseconds. The 7 ps component represents primarily the rise of the RP1 population. It thus reflects the *apparent lifetime* for primary charge separation, which is at least a factor of 5 faster than believed previously (*10*). The 10 ps component is a mixed component that cannot be assigned exclusively to one process. The energy transfer between the not directly connected CP43 and CP47 antennae makes a strong contribution, as does the rise of RP1. The 42 ps component is the dominant excited-state decay component (all three excited-state compartments contribute with decay terms to this component), and it also reflects the main rise of the RP2 population. RP1 and RP2 have been identified as representing the radical pair states $Chl_{acc\ D1}{}^{+}$ $Pheo_{D1}{}^{-}$ and $P_{D1}{}^{+}$ $Pheo_{D1}{}^{-}$, respectively (*14*). The 351 ps component reflects the rise of the RP trap state, which in analogy with previous data (*9*, *14*) represents the state $Pheo_{D1}{}^{+}$ $Q_A{}^{-}$.

The SAS of the excited states of the antenna complexes CP43 and CP47 have their emission peaks around 685 nm. The emission spectrum (SAS) of the excited RC state in an intact PS II core is resolved here for the first time. It peaks between 683 and 685 nm and has more than twice the amplitude of the SAS of the antenna complexes. The area under an SAS being proportional to the radiative transition probability of the corresponding state implies that the radiative rate of the RC* state is by a factor of 2−3 higher than that of the antenna excited states. This higher rate reflects, and is consistent with, the well-known increase of transition probability due to exciton coupling of the lower exciton states of the RC complex (*26*, *27*). It is interesting to compare the SAS of the RC* state to the one obtained earlier for the isolated D1-D2-cyt_{b559} complex, which is very similar in shape and also substantially higher in amplitude than the SAS of the peripheral monomeric Chl_z molecules in the D1-D2 RC (*16*). Thus, in both the intact PS II cores and the isolated D1-D2 RC the transition probability of the emitting exciton states of the RC is by a factor of 2−3 higher than for a monomeric Chl. However, the maximum of the RC emission in intact PS II cores seems to be red-shifted by ≈2 nm as compared to isolated D1-D2 RCs (*16*). It is also worth mentioning that the SAS of the RC shows a pronounced shoulder on the long-wavelength tail around 693

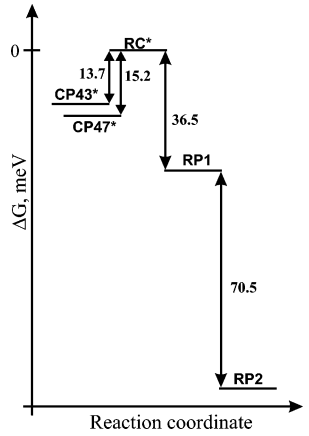

FIGURE 5: Scheme of free energy differences ΔG between the model compartments. The free energy of the RC excited state is used as thermodynamic reference.

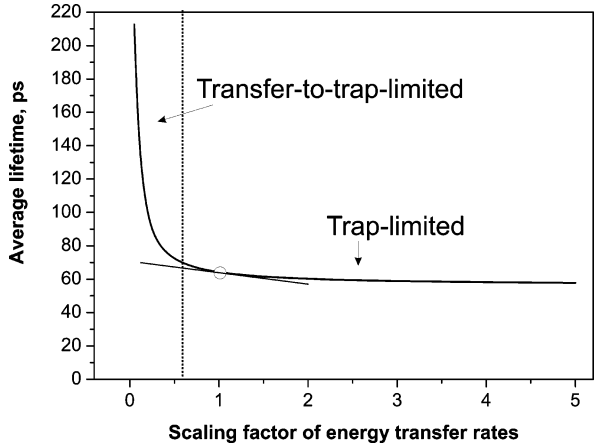

FIGURE 6: Dependence of the excited-state average lifetime $\tau_{\text{tot trap}}$ on the scaling of the energy-transfer rates given in the kinetic model (see Figure 2).

nm, and the spectrum shows substantial amplitude well above 700 nm. It is possible that the long-wavelength tail is caused by emission from low-lying emitting states, either exciton states or even charge-transfer states with significant optical transition probability. The presence of the latter states has recently been proposed for the isolated D1-D2 RC on the basis of exciton calculations (*28*).

From the rate constants of forward and reverse electron transfer in Figure 2 one can calculate the free energy differences between the excited RC* state and the radical pairs shown in Figure 5. The drop in ΔG for RP1 is -37 meV and between RP1 and RP2 is -71 meV, resulting in a total free energy drop of slightly less than -110 meV for the state RP2. Thus, the main energy drop occurs in the second electron-transfer process.

Trap versus Transfer-to-the-Trap Limit. The main energy-transfer lifetime between antenna and RC is 1.5 ps, with some small contribution of the 7 ps component to the rise of the RC* population (vide supra). In addition, the 10 ps component contributes with a small amplitude to energy equilibration between CP43 and CP47. The overall very fast energy transfer between antenna and RC is reflected in the fact that after antenna excitation the population of RC* reaches its maximal value at $\approx 4-5$ ps, whereas the RP1 state reaches its maximal population after ≈ 15 ps and the RP2 state after ≈ 100 ps. According to these data the energy transfer between antenna and RC (the transfer to the trap) is not rate-limiting for the overall charge separation process. Our results, which resolve for the first time the kinetics of energy transfer between the antenna and the RC directly, are in excellent agreement with the assumptions made previously in the derivation of the ERPE model (*9*).

The most transparent way of deciding upon the individual contributions of energy transfer (diffusion) and charge separation to the overall trapping process is the average lifetime of the decay of all excited states and their dependence on the rates of energy transfer and charge separation. The total average trapping time $\tau_{\text{tot trap}}$ as derived from theoretical work on energy transfer and trapping (*29*, *30*) is given by a sum of the individual contributions of diffusion within the antenna τ_{diff}, the transfer-to-the-trap (RC) time $\tau_{\text{transfer-to-trap}}$, and the charge separation time τ_{cs}, respectively. Because in our simple compartment model (Figure 2) we are not distinguishing between internal antenna diffusion and transfer to the trap processes, the relationship can be simplified to two terms as follows:

$$\tau_{\text{tot trap}} = \tau_{\text{diff}} + \tau_{\text{transfer-to-trap}} + \tau_{\text{cs}} = \tau_{\text{et}} + \tau_{\text{cs}}$$

Thus, τ_{et} represents the sum of the intra-antenna diffusion and transfer-to-the-trap times. The contributions of the charge separation time τ_{cs}, on the one hand, and the total energy transfer time τ_{et} to the total average trapping time, on the other hand, can be calculated easily within the kinetic model of Figure 2 by scaling up either the energy-transfer rates or the electron-transfer rates by a factor of >100, respectively. In this way the contributions of either τ_{et} or τ_{cs}, respectively, to the total trapping time are negligible and the value of the other term can be obtained. An alternative and equivalent way of obtaining τ_{cs} consists of solving the system of differential equations for the kinetic scheme with all of the initial excitation starting on the RC.

In a transfer-to-the-trap-limited kinetics the contribution of τ_{et} to the total trapping time is the dominant term, whereas in a trap-limited kinetics the τ_{cs} is the dominant term. Thus, in trap-limited kinetics the total trapping time depends only very weakly on the up-scaling of the energy-transfer rates. The dependence of the total trapping time (equivalent to the average excited-state decay lifetime) on the scaling of the energy-transfer rates in our model is shown in Figure 6. The scaling factor 1 corresponds to the experimental situation. As expected, the total trapping time depends only very weakly on the up-scaling of the energy-transfer rates, thus indicating a trap-limited overall kinetics for PS II cores. The calculation yields $\tau_{\text{tot trap}} = 65$ ps, $\tau_{\text{et}} = 9$ ps, and $\tau_{\text{cs}} = 56$ ps. With a ratio of $\tau_{\text{cs}}/\tau_{\text{et}} \geq 6$ the kinetics in PS II cores is on the extreme trap-limited side. This result is in vast disagreement with recent conclusions for the overall trapping kinetics in PS II cores to be transfer-to-the-trap-limited (*12*, *13*). The conclusions of Vasil'ev et al. claiming a transfer-to-the-trap-limited model result from a huge overestimation of the primary charge separation rate in PS II [rate constants for the primary charge separation process from P680 ranging from a minimum of 1400 ns^{-1} (*12*) to 7000 ns^{-1} (*11*) were reported] and a pronounced underestimation of the antenna to RC energy-transfer rates (*11*, *12*). Some of the likely reasons for the inadequacy of their estimated energy- and electron-transfer rates are revealed by their sequential radical

Table 1: Weighted Eigenvectors (Amplitude) of the Compartments for the Kinetic Model Shown in Figure 2[a]

lifetime, ps	compartment CP43*, excitation vector 0.9	compartment CP47*, excitation vector 0.1	compartment RC*, excitation vector 0	compartment RP1, excitation vector 0	compartment RP2, excitation vector 0	compartment RP trap, excitation vector 0
1.5	0.087	0.055	−0.198	0.068	−0.012	$5.9 \cdot 10^{-5}$
7	0.076	0.022	−0.009	−0.38	0.297	−0.006
10	0.354	−0.372	0.034	0.102	−0.122	0.004
42	0.352	0.366	0.156	0.144	−1.168	0.158
351	0.031	0.030	0.017	0.065	1.005	−1.143

[a] The time dependence of populations $C_j(t)$ for each intermediate compartment j (top row) follows the equation $C_j(t) = \sum_{i=1}^{n} A_{ij} \exp(-t/\tau_i)$, where A_{ij} represents the elements of the eigenvector matrix and τ_i are the lifetimes given in the left column. Inspection of this matrix allows one to easily deduce the *apparent lifetimes* and their amplitudes that contribute to the rise (negative amplitude) and decay (positive amplitude) of population of each of the intermediates (compartments). For further details of this presentation see Müller, M. G., Niklas, J., Lubitz, W., and Holzwarth, A. R. (2003) *Biophys. J.* 85, 3899−3922.

pair relaxation model (*11*). In that analysis the assumed intermediates RP1 to RP3 as well as the rate constants connecting P680* and these radical pairs are pure fitting artifacts that have no experimental foundation. This is clearly borne out by the fact that the fastest experimentally resolved lifetime component in the Vasil'ev data for PS II cores with open RC was 60 ps. This fastest lifetime can be obtained in their data by completely leaving out RP1−RP3 from the modeling. On the basis of the same arguments their conclusion of a significant radical pair relaxation contribution to the kinetics of PS II cores with open RCs lacks experimental support. We also note that there exists a severe discrepancy between the average lifetime of antenna decay of PS II cores with open RCs (F_0) in the measurements of Vasil'ev (*11*), which is 174 ps, and our average fluorescence decay lifetime with open centers of 65 ps (vide supra). The discrepancy is primarily caused by the significant contributions of 0.97 and 5 ns components in the fluorescence decay reported by Vasil'ev. These lifetime components according to our analysis are not related to PS II cores with intact open RCs but originate most likely from a contribution of closed RCs and/or damaged PS II particles. A non-negligible contribution of an 1.8 ns component to the fluorescence decay of PS II cores at F_0—also likely resulting from a contribution of PS II cores with closed RCs—was also found earlier by Schatz et al. (*10*). It requires very high sample purity and extreme care in avoiding multiple excitation of RCs closed by previous laser pulses in order to be able to achieve an experimental fluorescence decay that is essentially free of long-lived components in the range of 1 ns or longer.

Conclusions. The analysis of recent femtosecond transient absorption data of PS II cores with open RCs (*14*) and the analysis of the present fluorescence kinetic data show that both kinds of data can be described by the same kinetic model. The results presented here confirm the validity of the assumptions regarding energy equilibration made in deriving the earlier ERPE model for the trapping and charge separation kinetics in PS II cores (*9*, *10*). However, both the recent transient absorption data and the refined fluorescence kinetics reported here require an extension of the early ERPE model to include one additional electron-transfer step leading to an additional early radical pair. This first radical pair is the $Chl_{acc\ D1}^{+}$ $Pheo_{D1}^{-}$ state (*14*). Formation of this intermediate reflects itself in the fluorescence kinetics by an additional 7 ps component, which was not contained in the ERPE model. It is particularly gratifying that the same mechanism and also the same rates of the two early electron-transfer steps have been found for isolated PS II cores (this work and ref *14*) and for isolated D1-D2-cyt_{b559} RC (*14*).

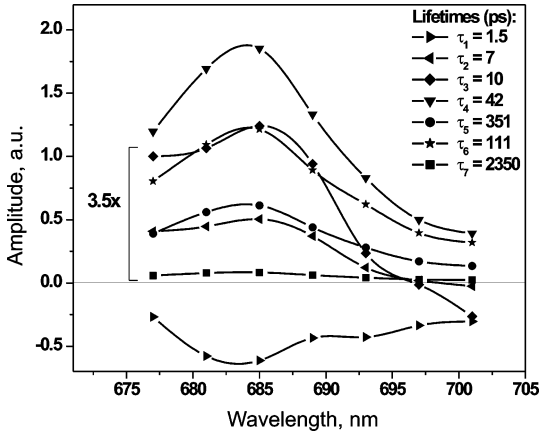

FIGURE 7: DAS from target analysis leading to the kinetic scheme shown in Figure 2. Lifetimes $\tau_1-\tau_5$ are those that result from the kinetic model. The 111 and 2350 ps lifetime components are additional free running components outside the kinetic scheme, which are required for a good fit.

This finding is in vast contrast to the claim of a ≈100-fold difference in the primary charge separation rate constants for isolated PS II RCs, on the one hand, and intact PS II cores, on the other (*11*).

ACKNOWLEDGMENT

We thank Michael Reus (Mülheim) and Claudia König and Bettina Thüner (Bochum) for excellent technical assistance. We also thank Hartmut Ulbrich and Stephan Syring (Mülheim) from the mechanical workshop for their dedication in developing the special rotation cuvette that made these measurements possible.

SUPPORTING INFORMATION AVAILABLE

Data for six- and five-component analyses. This material is available free of charge via the Internet at http://pubs.acs.org.

REFERENCES

1. Biesiadka, J., Loll, B., Kern, J., Irrgang, K.-D., and Zouni, A. (2004) Crystal structure of cyanobacterial photosystem II at 3.2 Å resolution: a closer look at the Mn-cluster, *Phys. Chem. Chem. Phys. 6*, 4733−4736.
2. Zouni, A., Witt, H. T., Kern, J., Fromme, P., Krauss, N., Saenger, W., and Orth, P. (2001) Crystal structure of photosystem II from *Synechococcus elongatus* at 3.8 Å resolution, *Nature 409*, 739−743.
3. Kamiya, N., and Shen, J.-R. (2003) Crystal structure of oxygen-evolving photosystem II from T*hermosynechococcus vulcanus* at 3.7-Å resolution, *Proc. Natl. Acad. Sci. U.S.A. 100*, 98−103.

4. Barber, J., Ferreira, K., Maghlaoui, K., and Iwata, S. (2004) Structural model of the oxygen-evolving centre of photosystem II with mechanistic implications, *Phys. Chem. Chem. Phys. 6*, 4737−4742.
5. Ferreira, K. N., Iverson, T. M., Maghlaoui, K., Barber, J., and Iwata, S. (2004) Architecture of the photosynthetic oxygen-evolving center, *Science 303*, 1831−1838.
6. Rögner, M., Boekema, E. J., and Barber, J. (1996) How does photosystem 2 split water? The structural basis of efficient energy conversion, *Trends Biochem. Sci. 21*, 44−49.
7. Renger, G. and Holzwarth, A. R. (2005) Primary electron transfer, in *Photosystem II: The Light-Driven Water/Plastoquinone Oxido-Reductase in Photosynthesis* (Wydrzynski, T., and Satoh, K., Eds.) pp 139−175, Springer, Dordrecht, The Netherlands.
8. Nuijs, A. M., van Gorkom, H. J., Plijter, J. J., and Duysens, L. N. M. (1986) Primary-charge separation and excitation of chlorophyll *a* in photosystem II particles from spinach as studied by picosecond absorbance-difference spectroscopy, *Biochim. Biophys. Acta 848*, 167−175.
9. Schatz, G. H., Brock, H., and Holzwarth, A. R. (1988) A kinetic and energetic model for the primary processes in photosystem II, *Biophys. J. 54*, 397−405.
10. Schatz, G. H., Brock, H., and Holzwarth, A. R. (1987) Picosecond kinetics of fluorescence and absorbance changes in photosystem II particles excited at low photon density, *Proc. Natl. Acad. Sci. U.S.A. 84*, 8414−8418.
11. Vassiliev, S., Lee, C.-I., Brudvig, G. W., and Bruce, D. (2002) Structure-based kinetic modeling of excited-state transfer and trapping in histidine-tagged photosystem II core complexes from *Synechocystis*, *Biochemistry 41*, 12236−12243.
12. Vasil'ev, S., Orth, P., Zouni, A., Owens, T. G., and Bruce, D. (2001) Excited-state dynamics in photosystem II: Insights from the X-ray crystal structure, *Proc. Natl. Acad. Sci. U.S.A. 98*, 8602−8607.
13. Dekker, J. P., and van Grondelle, R. (2000) Primary charge separation in Photosystem II, *Photosynth. Res. 63*, 195−208.
14. Holzwarth, A. R., Müller, M. G., Reus, M., Nowaczyk, M., Sander, J., and Rögner, M. (2006) Mechanism of electron transfer in intact photosystem II and in isolated reaction centers. Pheophytin is the primary electron acceptor, *Proc. Natl. Acad. Sci. U.S.A. 102*, in press.
15. Andrizhiyevskaya, E. G., Frolov, D., van Grondelle, R., and Dekker, J. P. (2004) On the role of the CP47 core antenna in the energy transfer and trapping dynamics of photosystem II, *Phys. Chem. Chem. Phys. 6*, 4810−4819.
16. Gatzen, G., Müller, M. G., Griebenow, K., and Holzwarth, A. R. (1996) Primary processes and structure of the photosystem II reaction center: III. Kinetic analysis of picosecond energy transfer and charge separation processes in the D1-D2-cyt-b_{559} complex measured by time-resolved fluorescence, *J. Phys. Chem. 100*, 7269−7278.
17. Holzwarth, A. R. (2004) Light absorption and harvesting, in *Molecular to Global Photosynthesis* (Archer, M. D., and Barber, J., Eds.) pp 43−115, Imperial College Press, London, U.K.
18. Kuhl, H., Kruip, J., Seidler, A., Krieger-Liszkay, A., Bunker, M., Bald, D., Scheidig, A. J., and Rögner, M. (2000) Towards structural determination of the water-splitting enzyme. Purification, crystallization, and preliminary crystallographic studies of photosystem II from a thermophilic cyanobacterium, *J. Biol. Chem. 275*, 20652−20659.
19. Müller, M. G., Griebenow, K., and Holzwarth, A. R. (1992) Primary processes in isolated bacterial reaction centers from *Rhodobacter sphaeroides* studied by picosecond fluorescence kinetics, *Chem. Phys. Lett. 199*, 465−469.
20. Holzwarth, A. R., Müller, M. G., Niklas, J., and Lubitz, W. (2005) Charge recombination fluorescence in photosystem I reaction centers from *Chlamydomonas reinhardtii*, *J. Phys. Chem. B 109*, 5903−5911.
21. Holzwarth, A. R. (1996) Data analysis of time-resolved measurements, in *Biophysical Techniques in Photosynthesis. Advances in Photosynthesis Research* (Amesz, J., and Hoff, A. J., Eds.) pp 75−92, Kluwer Academic Publishers, Dordrecht, The Netherlands.
22. Müller, M. G., Drews, G., and Holzwarth, A. R. (1993) Excitation transfer and charge separation kinetics in purple bacteria: 1. Picosecond fluorescence of chromatophores from *Rhodobacter capsulatus* wild type, *Biochim. Biophys. Acta 1142*, 49−58.
23. Groot, M.-L., Frese, R. N., de Weerd, F. L., Bromek, K., Pettersson, A., Peterman, E. J. G., van Stokkum, I. H. M., van Grondelle, R., and Dekker, J. P. (1999) Spectroscopic properties of the CP43 core antenna protein of photosystem II, *Biophys. J. 77*, 3328−3340.
24. Groot, M.-L., Peterman, E. J. G., van Stokkum, I. H. M., Dekker, J. P., and van Grondelle, R. (1995) Triplet and fluorescing states of the CP47 antenna complex of photosystem II studied as a function of temperature, *Biophys. J. 68*, 281−290.
25. de Weerd, F. L., van Stokkum, I. H. M., van Amerongen, H., Dekker, J. P., and van Grondelle, R. (2002) Pathways for energy transfer in the core light-harvesting complexes CP43 and CP47 of photosystem II, *Biophys. J. 82*, 1586−1597.
26. Durrant, J. R., Klug, D. R., Kwa, S. L., van Grondelle, R., Porter, G., and Dekker, J. P. (1995) A multimer model for P680, the primary electron donor of photosystem II, *Proc. Natl. Acad. Sci. U.S.A. 92*, 4798−4802.
27. Prokhorenko, V. I., and Holzwarth, A. R. (2000) Primary processes and structure of the photosystem II reaction center: a photon echo study, *J. Phys. Chem. B 104*, 11563−11578.
28. Novoderezhkin, V. I., Andrizhiyevskaya, E. G., Dekker, J. P., and van Grondelle, R. (2005) Pathways and timescales of primary charge separation in the photosystem II reaction center as revealed by a simultaneous fit of time-resolved fluorescence and transient absorption, *Biophys. J. 89*, 1464−1481.
29. van Grondelle, R., and Gobets, B. (2004) Transfer and trapping of excitations in plant photosystems, in *Chlorophyll a Fluorescence: A Signature of Photosynthesis* (Papageorgiou, G. C., and Govindjee, Eds.) pp 107−132, Springer, Dordrecht, The Netherlands.
30. Pearlstein, R. M. (1982) Chlorophyll singlet excitons, in *Photosynthesis. Vol. 1 Energy Conversion by Plants and Bacteria* (Govindjee, Ed.) pp 293−331, Academic Press, New York.

BI052248C